**Rare Metal Materials and Engineering**
Volume 46, Issue 1, January 2017
Online English edition of the Chinese language journal

Available online at www.sciencedirect.com
ScienceDirect

**Cite this article as:** Rare Metal Materials and Engineering, 2017, 46(1): 0078-0082.

ARTICLE

# Electrochemical Performance of $LiMnBO_3$/C Composite Synthesized by Wet Impregnating Method

**Tang Anping[1], He Zeqiang[2], Xu Guorong[1], Peng Ronghua[1], Song Haishen[1]**

*[1] Key Laboratory of Theoretical Organic Chemistry and Function Molecule, Ministry of Education, Hunan University of Science and Technology, Xiangtan 411201, China; [2] Jishou University, Jishou 416000, China*

**Abstract:** Hexagonal-$LiMnBO_3$/C composite was prepared by a wet impregnating method using the 3D-network ketchen black (KB) as both a temple and a conductive framework. The crystal structure, morphology and specific surface area were characterized by X-ray diffraction, scanning electron microscopy and nitrogen sorption measurements, respectively. The electrochemical properties of the composite were studied by galvanostatic charge/discharge and cyclic voltammetry measurements. Results show that when tested at C/20 rate for Li ion insertion/extraction properties, $LiMnBO_3$/C composite exhibits good cycle capability with discharge capacity retention of 87.4% at the 30th cycle. As the current rate increases from C/20, C/10 to C/5, good rate capability is obtained for all rates with initial discharge specific capacities of 138.8, 124.5 and 100.5 mAh $g^{-1}$, respectively.

**Key words:** $LiMnBO_3$; lithium ion batteries; cathode

Lithium metal borates (Li*M*$BO_3$, *M*=Mn, Fe, Co) have been recently reported as promising alternative cathodes for lithium-ion battery due to their high theoretical specific capacity (~220 mAh $g^{-1}$), thermal stability, electrochemical stability and environmentally benign nature[1-8]. Among the above borates, $LiMnBO_3$ generally exists in two structures, namely the monoclinic structure and the hexagonal structure, and has higher energy density along with high redox voltage (4.1 V/3.7 V) compared to $LiFeBO_3$. However, the lithium metal borates in general suffer from poor electronic conductivity, $Li^+$ diffusivity and Li-blockage by anti-site defects, poor electronic and ionic conductivity similar to those of the olivine framework[1,9,10]. Recently, these obstacles have been overcome for Li*M*$BO_3$ by employing conductive carbon coatings, nano-sizing and preventing the surface poisoning of the materials in recent studies[2, 3, 11-13], particularly in the case of $LiFeBO_3$. The series of work presents new possibilities for the development of cathodes made with Li*M*$BO_3$ that have both high energy density and stability. In comparison to $LiFeBO_3$, $LiMnBO_3$ is an attractive cathode material owing to its higher $Li^+$ intercalation potential of 3.7 V for monoclinic $LiMnBO_3$ and 4.1 V for hexagonal $LiMnBO_3$ (3.0 V for $LiFeBO_3$), providing higher theoretical energy density than $LiFeBO_3$. Nevertheless, these adverse effects such as poor electronic conductivity and $Li^+$ diffusivity are more prominent in case of $LiMnBO_3$ with very higher energy barrier in Li-ion channels than in case of $LiFeBO_3$, making it challenging to achieve high capacity for $LiMnBO_3$ using methods developed for $LiFeBO_3$[1,9-11,14]. Thus, only a smaller fraction of the theoretical capacity of $LiMnBO_3$ could be accessed up to date[1,13-16].

In the present investigation, $LiMnBO_3$/C composite was synthesized by a wet impregnating method using 3D-network KB as both a template and a conductive framework. The templating function of KB can be attributed to its unique properties, such as the 3D connectivity of the pore system, high pore volume and narrow pore size distribution, which can control the particle size of $LiMnBO_3$ and the morphology of $LiMnBO_3$/KB composite. The conductive framework function of KB can be attributed to the continuous and connected nano

Received date: December 6, 2015
Foundation item: National Natural Science Foundation of China (51262008, 51202087); Hunan Provincial Natural Science Foundation of China (12JJ2022); Scientific Research Fund of Hunan Provincial Education Department (14A052)
Corresponding author: Tang Anping, Ph. D., Associate Professor, School of Chemistry and Chemical Engineering, Hunan University of Science and Technology, Xiangtan 411201, P. R. China, Tel: 0086-731-58290045, E-mail: 535953632@qq.com

carbon particles. Additionally, the structure and the electrochemical performance of $LiMnBO_3$/C composite were also characterized.

## 1 Experiment

All chemicals were of analytical grade from Kemiou Chemical Reagent Company (Tianjin, China) except KB (Lion Corporation Limited). In a typical synthesis, 0.02 mol $CH_3COOLi{\cdot}2H_2O$ and 0.02 mol $Mn(CH_3COO)_2{\cdot}4H_2O$ were dissolved in 30 mL absolute alcohol at 50 °C for 30 min, and similarly, 0.02 mol tributyl borate in 20 mL absolute alcohol. After the salts were completely dissolved, the two solutions were mixed and violently stirred for 1 h at 50 °C. After 0.2099 g of KB was impregnated with the above solution, 2 mL water was added for hydrolysis and a powder was obtained by evaporating the solvent at 50~70 °C. Finally, hexagonal-$LiMnBO_3$/C composite was obtained after heating the powder in a tube furnace at 500 ℃ for 10 h under flowing argon.

Powder X-ray diffractions (XRD) pattern was obtained on a D8 Advance type diffractometer equipped with Cu Kα radiation (operated at 40 kV, 40 mA). The XRD pattern was analyzed with MDI Jade 5.0 software to identify phase and to calculate lattice parameters. The surface morphology of the samples was observed using a JSM-6380 scanning electron microscopy (SEM). The CHN Elemental analyzer was used to measure the amount of residual carbon in the $LiMnBO_3$/C composite material. The surface areas and pore volumes of samples were determined via nitrogen sorption with a Micromeritics ASAP 2020 adsorption porosimeter at 77 K. The surface area and pore volumes were calculated using the Brunauer-Emmet-Teller (BET) method and the Barrett-Joyner-Halenda (BJH) method, respectively.

For electrochemical studies, composite electrodes were fabricated with the active material, conductive carbon (acetylene black+ketchen black+in-situ carbon) and binder (polyvinylidene fluoride) in the mass ratio 70:20:10 using N-methyl pyrrolidone as a solvent. Electrodes were prepared using an etched aluminium foil as a current collector by the doctor-blade technique. Lithium metal foil, 1 mol/L $LiPF_6$ solution in ethylene carbonate-diethyl carbonate (EC-DEC, 3/7, volume ratio) and Celgard 2502 membrane were used as a counter electrode, electrolyte and separator, respectively to assemble coin-type cells (size 2025) in an Ar-filled glove box (Mikrouna). The active material content in the electrode was around 3~5 mg. Galvanostatic tests were done in the voltage range of 4.5~1.7 V with constant voltage charge at 4.5 V until the current decay below 2 mA $g^{-1}$. Cyclic voltammetry (CV) tests were carried out at various scan rates within 4.5~1.7 V using a computer controlled CHI660C electrochemical analyzer.

## 2 Results and Discussion

Structural analysis of $LiMnBO_3$/C composite sintered at 500 °C for 10 h was investigated by XRD studies. The XRD pattern of the sample, shown in Fig.1, is similar to the previous reports[1,17]. The diffraction peaks of the sample correspond to a single-phase and no other secondary phases are detected. Unit cell parameters of $a$=0.8178 nm and $c$= 0.3146 nm were determined by Jade 5.0 software, consistent with literature values described elsewhere[1]. Although the residual carbon content in the $LiMnBO_3$/C composite is 10.4% in mass measured by CHN analyzer, there is no obvious carbon diffraction peaks in the profile of the composite because the residual carbon including KB and the carbon from the pyrolysis of acetate is amorphous.

Fig.2 shows the $N_2$ adsorption/desorption isotherms for KB and the $LiMnBO_3$/C composite. The $N_2$ adsorption-desorption isotherms shows a strong hysteresis loop, which is an adsorption-desorption characteristic of the porous materials. Furthermore, the inflection point in the isotherm for $LiMnBO_3$/C showing a shift to a smaller relative pressure proves that the mesopore of KB is filled or blocked by $LiMnBO_3$, resulting in a reduced surface area, pore volume and pore size. A comparison on pore structure parameters of KB and the $LiMnBO_3$/C composite is listed in Table 1. As listed in Table 1, the BET surface area, pore volume and pore size drop from 1290 $m^2\ g^{-1}$, 2.47 $cm^3\ g^{-1}$ and 11.85 nm for KB to 78.7 $m^2\ g^{-1}$, 0.18 $cm^3\ g^{-1}$ and 8.83 nm for the $LiMnBO_3$/C composite, which affirm the impregnation of $LiMnBO_3$ in KB inner pores.

The morphologies of the $LiMnBO_3$/C composite and KB observed via SEM are shown in Fig.3. The nanostructured carbon network of KB can be clearly observed in Fig.3b. The $LiMnBO_3$ particles uniformly disperse inside the KB network. There are generally two possible locations of $LiMnBO_3$ guest particles in the KB matrix. The guest particles may be located inside the inner pores or at the external surface of the KB. In this investigation, it seems that some agglomerated and bigger $LiMnBO_3$ particles are on the external surface of KB; however, based on BET results most of the inner pores are filled by smaller $LiMnBO_3$ particles. The average sizes of agglomerated $LiMnBO_3$ particles which are estimated from SEM images are between 0.1 and 0.3 μm.

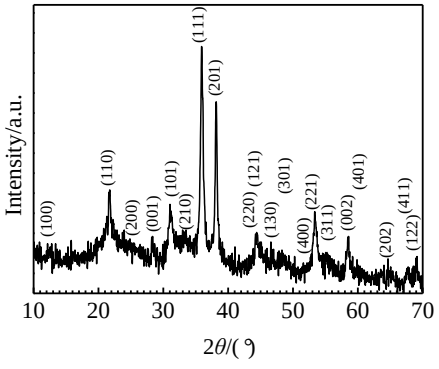


Fig.1 XRD pattern of $LiMnBO_3$/C composite

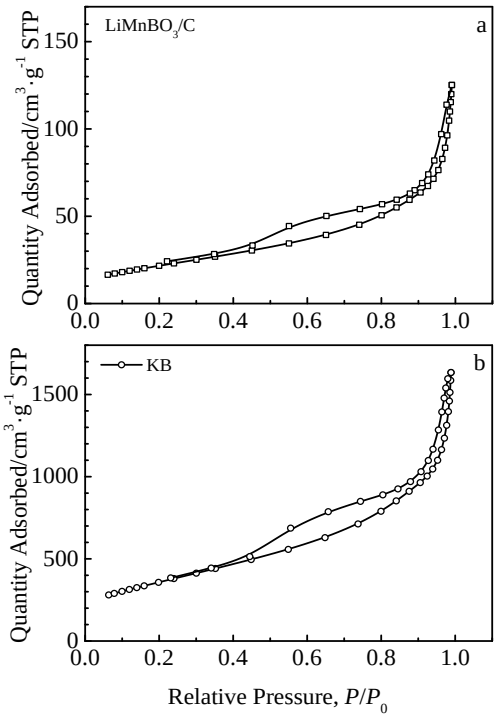


Fig.2 Nitrogen adsorption-desorption isotherms of the $LiMnBO_3$/C composite (a) and KB (b)

**Table 1 Pore volumes and BET surface areas of KB and the $LiMnBO_3$/C composite**

| Sample | KB | $LiMnBO_3$/C |
|---|---|---|
| $S_{BET}$/$m^2$ $g^{-1}$ | 1290 | 78.7 |
| Pore volume/$cm^3$ $g^{-1}$ | 2.47 | 0.18 |
| Pore size/nm | 11.85 | 8.83 |

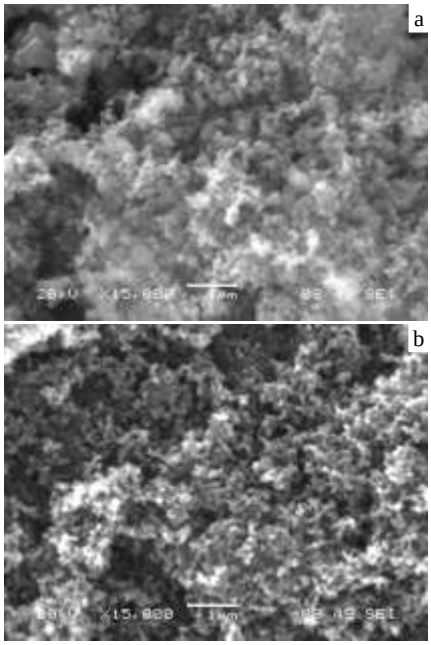


Fig.3 SEM images of $LiMnBO_3$/C composite (a) and KB (b)

The first five charge/discharge curves for the $LiMnBO_3$/C composite are displayed in Fig.4. The cells were cycled under a C/20 (1 C=222 mAh $g^{-1}$) rate in the voltage range between 1.5 and 4.5 V with constant voltage charge at 4.5 V until the current decays below 2 mA $g^{-1}$. Charge and discharge curves have undergone continuous change through the capacity, namely, no noticeable plateau is observed, in accordance with the previous report[17, 18], indicating that (de)lithiation occurs through a solid solution mechanism. The significant difference occurs between the first charge potential curve and the subsequent ones, which are also present for $LiCoBO_3$ and $LiFeBO_3$[2, 7, 19]. These differences could be explained by the partial amorphization of $LiMnBO_3$ due to the stress induced after the first cycle[17]. Besides, the charge and discharge process has a high degree of polarization, for example, the average voltage for charge is found to be ~3.9 V vs $Li^+$/Li after the first cycle, whereas the average discharge voltage is approximately 2.9 V vs $Li^+$/Li. This huge polarization shows the poor kinetics in the system that is very similar to the cases of $LiFeBO_3$ and $LiCoBO_3$. The composite delivers an initial capacity of 138.7 mAh $g^{-1}$ with a charge/discharge efficiency of 90.7%.

Further investigation into the composite's performance was carried out by examining the effect of current rate on the capacity of the composite. Fig.5 shows the reversible capacity of the composite obtained at different current rates like C/20, C/10 and C/5. It can be found that the composite exhibits good rate capability with initial discharge specific capacities of 138.8 mAh $g^{-1}$ (C/20), 124.5 mAh $g^{-1}$ (C/10) and 100.5 mAh $g^{-1}$ (C/5). Although the first discharge specific capacity of 138.8 mAh $g^{-1}$ at C/20 is lower than the theoretical value and that reported by Afyon et al[17], it is much higher than those of the solid-state reaction or spray-drying process[15,20,21]. In the papers reported by Chen[15], Li[20] and Lee[21] h-$LiMnBO_3$ showed the first discharge capacity of 75.5 mAh $g^{-1}$ in the voltage range between 1~4.8 V, 90.7 mAh $g^{-1}$ within 1.25~4.80 V and 53 mAh $g^{-1}$ in the voltage range between 1.5~4.5 V at C/20, respectively. Moreover, the composite exhibits good cycling performance at all the three current

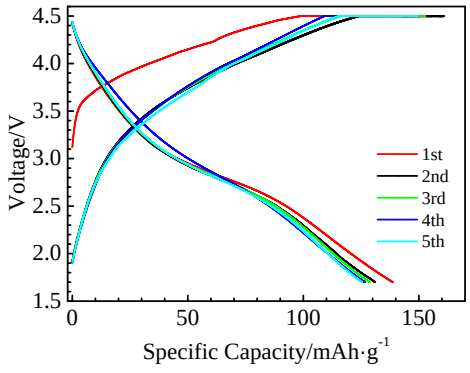


Fig.4 First five charge/discharge curves of $LiMnBO_3$/C composite within 4.5~1.5 V at C/20 rate

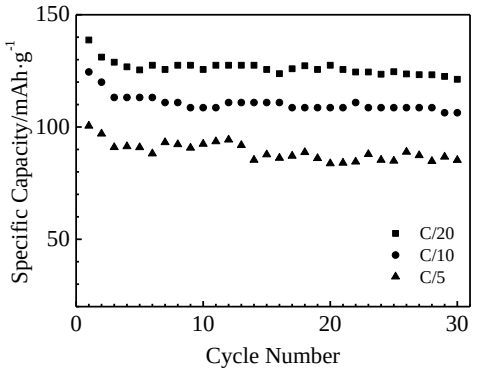


Fig.5 Discharge specific capacity vs cycle number at various current rates

rates. For example, the discharge specific capacity is 121.3 mAh $g^{-1}$ with discharge capacity retention of 87.4% at the 30th cycle under C/20, which is higher than that reported by Aravindan[16] and by Li et al[20] for hexagonal $LiMnBO_3$/C cycled at C/20. Considering the low conducting nature of the $LiMnBO_3$, this result is a significant improvement compared to the earlier work with various rates[15,16]. The enhanced properties for the $LiMnBO_3$/C composite may be attributed to the covering and connecting of active $LiMnBO_3$ by KB that is expected to facilitate electron and lithium ion transport.

Fig.6 shows the CVs for the $LiMnBO_3$/C composite, which were recorded using the Li metal as counter and reference electrodes in the voltage range of 4.5~1.7 V at the scan rate of 0.08 mV $s^{-1}$. In all cycles, no obvious oxidation peaks are observed in the oxidation process; they instead exhibit a gently upward slope from 2.8 to 4.2 V, except the first oxidation step, in which a broad oxidation peak occurs at ~3.68 V vs. $Li/Li^+$. A broad reduction peak is observed around 2.8 V in each cycle, ranging from ~3.5 to 2.4 V, indicating CV curves of $LiMnBO_3$ without sharp and symmetrical redox peaks, perhaps due to its low electrical conductivity, small Li-ion diffusivity and a solid solution mechanism. The reduction peak intensities have dropped slightly at each cycle, consistent with the capacity loss observed in the charge and discharge curves. However, the peak positions approximately remain unchanged which may be interpreted as reversible insertion/extraction mechanisms.

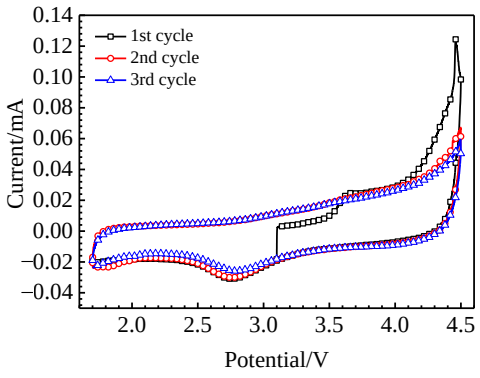


Fig.6 CV profiles of the $LiMnBO_3$/C composite at the scan rate of 0.08 mV $s^{-1}$

CV of the $LiMnBO_3$/C composite was also carried out at various scan rates. Fig.7 shows the CV profiles of the composite in the scan rate range of 0.02~0.16 mV $s^{-1}$. The reduction peak separation and reduction peak intensity change as a function of the scan rate. For the coin-type cell systems the electrodes can approximately be regarded as a flat one[22], and the relationship between the peak current and the scan rate is represented as follows:

$$i_p=2.69\times10^5 n^{3/2}Av^{1/2}D^{1/2}C_0 \quad (1)$$

where $i_p$ is the peak current (A), $C_0$ is the initial concentration of Li ion (mol/$cm^3$), $v$ is scan rate (V $s^{-1}$), $A$ is electrode area ($cm^2$) and $D$ is the diffusion constant ($cm^2$ $s^{-1}$)[23]. The reduction peak current from Fig.7 is plotted in Fig. 8 vs the square root of the scan rates, as expected for diffusion-controlled process. The peak current shows a half-order dependence on the scan rate, consistent with semi-infinite diffusion control, for the entire range of scan rates. From the slope of $i_p$ vs $v^{1/2}$, the diffusion coefficient of lithium ion in $LiMnBO_3$ has been estimated. The diffusion coefficient of lithium ion is $1.04\times10^{-13}$ $cm^2$ $s^{-1}$, which is higher by 2 orders of magnitude than the value measured by electrochemical impedance spectroscopy[20], but is lower by 2 orders of magnitude than the computational result[9].

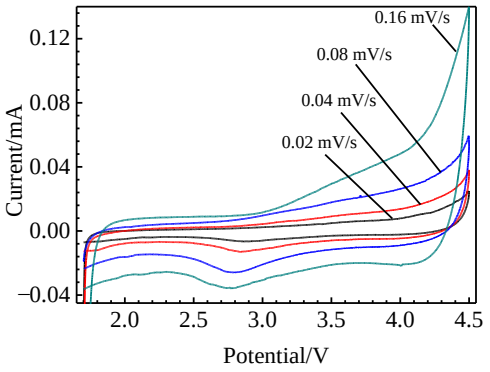


Fig.7 CV profiles of the $LiMnBO_3$/C composite at different scan rates

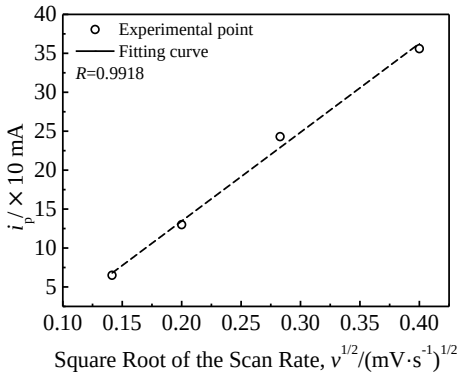


Fig.8 Plot of reduction peak current vs square root of the scan rate

## 3 Conclusions

1) Hexagonal $LiMnBO_3$/C composite can be synthesized by the wet impregnating method.

2) The $LiMnBO_3$/C composite exhibits good cycle capability at all the three current rates of C/20, C/10 and C/5.

3) The $LiMnBO_3$/C composite shows good rate capability with initial discharge specific capacities of 138.8 mAh $g^{-1}$ (C/20), 124.5 mAh $g^{-1}$ (C/10) and 100.5 mAh $g^{-1}$ (C/5).

## References


1 Legagneur V, An Y, Mosbah A *et al*. *Solid State Ionics*[J], 2001, 139(1-2): 37

2 Yamada A, Iwane N, Harada Y *et al*. *Adv Mater*[J], 2010, 22: 3583

3 Bo S H, Wang F, Janssen Y *et al*. *J Mater Chem*[J], 2012, 22: 8799

4 Kim J C, Moore C J, Kang B *et al*. *J Electrochem Soc*[J], 2011, 158: 309

5 Liu G Q, Wu Q Y, Ma B Y. *Adv Mater Res*[J], 2011, 197-198: 526

6 Yamashita Y, Barpanda P, Yamada Y *et al*. *Electrochem Lett*[J], 2013, 2(8): 75

7 Afyon S, Mensing C, Krumeich F *et al*. *Solid State Ionics*[J], 2014, 256: 103

8 Tao L, Rousse G, Chotard J N *et al*. *J Mater Chem A*[J], 2014, 2: 2060

9 Seo D H, Park Y U, Kim S W *et al*. P*hys Rev B*[J], 2011, 83: 205 127-1

10 Lin Z P, Zhao Y J, Zhao Y M. *Phys Letts A*[J], 2012, 376: 179

11 Allen J L, Xu K, Zhang S S *et al*. *Mat Res Soc Symp Proc*[J], 2002, 730: 9

12 Dong Y Z, Zhao Y M, Fu P *et al*. *J Alloy Compd*[J], 2008, 461: 585

13 Dong Y Z, Zhao Y M, Shi Z D *et al*. *Electrochim Acta*[J], 2008, 53: 2339

14 Kim J C, Moore C J, Kang B *et al*. *J Electrochem Soc*[J], 2011, 158: 309

15 Chen L, Zhao Y M, An X N *et al*. *J Alloy Compd*[J], 2010, 494: 415

16 Aravindan V, Karthikeyan K, Amaresh S *et al*. *Bull Korean Chem Soc*[J], 2010, 31: 1506

17 Afyon S, Kundu D, Krumeich F *et al*. *J Power Sources*[J], 2013, 224: 145

18 Yamada A, Iwane N, Nishimura S I *et al*. *J Mater Chem*[J], 2011, 21: 10690

19 Aravindan V, Umadevi M. *Ionics*[J], 2012, 18: 27

20 Li S L, Xu L Q, Li G D *et al*. *J Power Sources*[J], 2013, 236: 54

21 Lee K J, Kang L S, Uhm S *et al*. *Current Applied Physics*[J], 2013, 13: 1440

22 Ren M M, Zhou Z, Su L W *et al*. *J Power Sources*[J], 2008, 189: 786

23 Bard A J, Faulkner L R. *Electrochemical Methods: Fundamentals and Applications*[M]. Hoboken: John Wiley& Sons, 1980: 213


# 湿浸渍法合成 $LiMnBO_3$/C 复合材料及其电化学性能


唐安平[1]，何则强[2]，徐国荣[1]，彭荣华[1]，宋海申[1]

(1. 湖南科技大学 理论有机化学与功能分子教育部重点实验室，湖南 湘潭 411201)

(2. 吉首大学，湖南 吉首 416000)



**摘 要**：以三维网络结构的科琴黑(KB)为模板和导电骨架，采用湿浸渍法合成了六方结构的 $LiMnBO_3$/C 复合材料。用 X 射线衍射、扫描电镜和氮吸附等测试技术分别对样品的微观结构、形貌和比表面积进行了表征。用恒流充放电和循环伏安对复合材料的电化学性能进行了研究。当 $LiMnBO_3$/C 复合材料以 C/20 倍率进行锂离子脱嵌性能测试时，30 周循环后放电容量保持率为 87.4%，表现出优良的循环稳定性。当电流从 C/20、C/10 增至 C/5 时，复合材料的首次放电比容量依次为 138.8、124.5 和 100.5 mAh $g^{-1}$，表明复合材料具有良好的倍率性能。



**关键词**：$LiMnBO_3$；锂离子电池；正极



作者简介：唐安平，男，1969 年生，博士，副教授，湖南科技大学化学化工学院，湖南 湘潭 411201，电话：0731-58290045，E-mail: 535953632@qq.com